

Silver(I) Complexes in Coordination Supramolecular System with Bulky Acridine-Based Ligands: Syntheses, Crystal Structures, and Theoretical Investigations on C–H...Ag Close Interaction

Chun-Sen Liu,[†] Pei-Quan Chen,[‡] En-Cui Yang,[§] Jin-Lei Tian,[†] Xian-He Bu,^{*,†} Zheng-Ming Li,^{*,†} Hong-Wei Sun,[†] and Zhenyang Lin^{||}

Department of Chemistry and Institute of Elemento-Organic Chemistry and State Key Laboratory of Elemento-Organic Chemistry, Nankai University, Tianjin 300071, College of Chemistry & Life Science, Tianjin Normal University, Tianjin 300074, and Department of Chemistry, The Hong Kong University of Science and Technology, Kowloon, Hong Kong, P. R. China

Received January 17, 2006

In our efforts to investigate the coordination architectures of transition metals and organic ligands with tailored structures, we have prepared two structurally related rigid bulky acridine-based ligands, 9-[3-(2-pyridyl)pyrazol-1-yl]-acridine (**L**¹) and 9-(1-imidazolyl)acridine (**L**²), and synthesized and characterized four of their Ag(I) complexes, {[AgL¹](ClO₄)₂}₂ (**1**), {[AgL¹](NO₃)₂}₂ (**2**), [AgL²](ClO₄) (**3**), and {[Ag₃L²](NO₃)}(NO₃)₂(H₂O)}_∞ (**4**). The single-crystal X-ray diffraction analysis shows that the structures of **1** and **2** are similar to each other, with the two intramolecular Ag(I) centers of each complex being encircled by two **L**¹ ligands; this forms a unique boxlike cyclic dimer, which is further linked to form one-dimensional (1D) chains of **1** and a two-dimensional (2D) network of **2** by intermolecular face-to-face $\pi\cdots\pi$ stacking and/or weak C–H...O hydrogen-bonding interactions, respectively. **3** has a mononuclear structure, which is further assembled into a 2D network via intermolecular Ag...O and $\pi\cdots\pi$ stacking weak interactions. **4** possesses two different 1D motifs that are further interlinked through interlayer face-to-face $\pi\cdots\pi$ stacking and Ag...O weak interactions, resulting in a 2D network. It is worth noting that one of the interesting structural features of **1**, **2**, and **4** is the presence of obvious C–H...M hydrogen-bonding interactions between the Ag centers and some acridine ring H atoms identified by X-ray diffraction on the basis of the van der Waals radii. Furthermore, as a representative example, full geometry optimization on the basis of the experimental structure, the natural bond orbital (NBO), and topological analysis of **1** were carried out by DFT and AIM (Atoms in Molecules) calculations. The total C–H...Ag interaction energy in **1** is estimated to be about 14 kJ/mol. Therefore, this work offers three new rare examples (**1**, **2**, and **4**) that exhibit C–H...Ag weak interactions, in which the N donors of the acridine rings coordinate to Ag(I) ions. Also, these results strongly support the existence of C–H...Ag close interactions and allow us to have a better understanding of the nature of such interactions in the coordination supramolecular systems.

Introduction

Nowadays, the rational design and synthesis of discrete polynuclear or polymeric coordination architectures has attracted great interest because of their interesting topologies and potential uses as functional materials.^{1–3} In these fields,

the selection of proper ligands as building blocks is usually a key factor in manipulating the structures of complexes.⁴ According to our previous work,^{5a–c} in comparison with

* To whom correspondence should be addressed. Fax: 86-22-23502458. E-mail: buxh@nankai.edu.cn (X.-H.B.); nkzml@nk.sina.net (Z.-M.L.).

[†] Department of Chemistry, Nankai University.

[‡] Institute of Elemento-Organic Chemistry, Nankai University.

[§] Tianjin Normal University.

^{||} The Hong Kong University of Science and Technology.

(1) For recent reviews, see (a) Kitagawa, S.; Kitaura, R.; Noro, S. *Angew. Chem., Int. Ed.* **2004**, *43*, 2334. (b) Ruben, M.; Rojo, J.; Romero-Salguero, F. J.; Uppadine, L. H.; Lehn, J.-M. *Angew. Chem., Int. Ed.* **2004**, *43*, 3644. (c) Yaghi, O. M.; O'Keeffe, M.; Ockwig, N. W.; Chae, H. K.; Eddaoudi, M.; Kim, J. *Nature* **2003**, *423*, 705. (d) Evans, O. R.; Lin, W. B. *Acc. Chem. Res.* **2002**, *35*, 511. (e) Seidel, S. R.; Stang, P. J. *Acc. Chem. Res.* **2002**, *35*, 972. (f) Gade, L. H. *Acc. Chem. Res.* **2002**, *35*, 575. (g) Moulton, B.; Zaworotko, M. J. *Chem. Rev.* **2001**, *101*, 1629. (h) Fujita, M. *Acc. Chem. Res.* **1999**, *32*, 53. (i) Steel, P. J. *Acc. Chem. Res.* **2005**, *38*, 243.

other heterocyclic N-donor ligands, acridine-based ligands have some primary structural characteristics: (1) the acridine ring has larger conjugated π -systems, therefore $\pi\cdots\pi$ stacking interactions may play important roles in the formations of their complexes; (2) the larger conjugated π -systems and the steric hindrance of H atoms of the adjacent benzene rings probably affect the coordination abilities of the acridine N donor. Until recently, therefore, it has been believed that the N donor of the acridine ring should have difficulty taking part in coordination because of the reasons mentioned above,⁵ especially for Ag(I) coordination complexes with different acridine-based ligands. To the best of our knowledge, only a few examples of the metal complexes with such ligands have been studied and reported to date.^{5d–g}

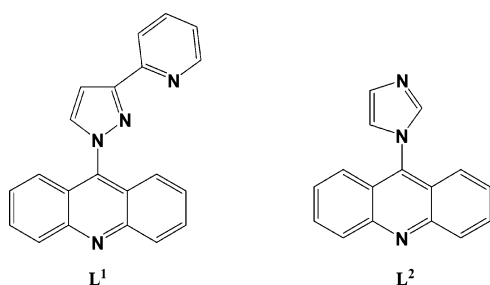
In addition to typical coordination bonds,^{5,6} weak intra- or intermolecular interactions such as some weak C–H···X close interactions (X is O, N, Cl, S, I, or some transition-metal ions, etc.)^{7–11} and $\pi\cdots\pi$ stacking^{12–14} interactions also often play crucial roles in metallosupramolecular compounds,

- (2) For examples: (a) Zhao, X.; Xiao, B.; Fletcher, A. J.; Thomas, K. M.; Bradshaw, D.; Rosseinsky, M. *J. Science* **2004**, *306*, 1012. (b) Schelter, E. J.; Prosvirnin, A. V.; Dunbar, K. R. *J. Am. Chem. Soc.* **2004**, *126*, 15004. (c) Rosi, N. L.; Eckert, J.; Eddaoudi, M.; Vodak, D. T.; Kim, J.; O'Keeffe, M.; Yaghi, O. M. *Science* **2003**, *300*, 1127. (d) Kesanli, B.; Cui, Y.; Smith, M. R.; Bittner, E. W.; Bockrath, B. C.; Lin, W. B. *Angew. Chem., Int. Ed.* **2005**, *44*, 72.
- (3) For examples: (a) Huang, X.-C.; Zhang, J.-P.; Lin, Y.-Y.; Yu, X.-L.; Chen, X.-M. *Chem. Commun.* **2004**, 1100. (b) Cao, R.; Sun, D. F.; Liang, Y. C.; Hong, M. C.; Tatsumi, K.; Shi, Q. *Inorg. Chem.* **2002**, *41*, 2087. (c) Carlucci, L.; Ciani, G.; Proserpio, D. M.; Porta, F. *Angew. Chem., Int. Ed.* **2003**, *42*, 317. (d) Oh, M.; Carpenter, G. B.; Sweigart, D. A. *Angew. Chem., Int. Ed.* **2003**, *42*, 2026. (e) Tong, M. L.; Wu, Y. M.; Ru, J.; Chen, X. M.; Chang, H. C.; Kitagawa, S. *Inorg. Chem.* **2002**, *41*, 4846. (f) Wu, C.-D.; Lu, C.-Z.; Lin, X.; Wu, D.-M.; Lu, S.-F.; Zhuang, H.-H.; Huang, J.-S. *Chem. Commun.* **2003**, 1284. (g) Sekiya, R.; Nishikiori, S. *Chem.—Eur. J.* **2002**, *8*, 4803. (h) Mao, Z.; Chao, H.-Y.; Hui, Z.; Che, C.-M.; Fu, W.-F.; Cheung, K.-K.; Zhu, N.-Y. *Chem.—Eur. J.* **2003**, *9*, 2885.
- (4) For examples: (a) Stang, P. J.; Zhdankin, V. V. *Chem. Rev.* **1996**, *96*, 1123. (b) Fujita, M. *Chem. Soc. Rev.* **1998**, *27*, 417. (c) Sharma, C. V. K.; Broker, G. A.; Huddleston, J. G.; Baldwin, J. W.; Metzger, R. M.; Rogers, R. D. *J. Am. Chem. Soc.* **1999**, *121*, 1137. (d) Kaes, C.; Katz, A.; Hosseini, M. W. *Chem. Rev.* **2000**, *100*, 3553. (e) Noro, S.; Kitaura, R.; Kondo, M.; Kitagawa, S.; Ishii, T.; Matsuzaka, H.; Yamashita, M. *J. Am. Chem. Soc.* **2002**, *124*, 2568. (f) Ye, B. H.; Tong, M. L.; Chen, X. M. *Coord. Chem. Rev.* **2005**, *249*, 545. (g) Lu, J.; Crisci, G.; Niu, T.; Jacobson, A. J. *Inorg. Chem.* **1997**, *36*, 5140.
- (5) (a) Bu, X.-H.; Tong, M.-L.; Chang, H.-C.; Kitagawa, S.; Batten, S. R. *Angew. Chem., Int. Ed.* **2004**, *43*, 192. (b) Bu, X.-H.; Tong, M.-L.; Li, J.-R.; Chang, H.-C.; Li, L.-J.; Kitagawa, S. *CrystEngComm* **2005**, *7*, 411. (c) Bu, X.-H.; Tong, M.-L.; Xie, Y.-B.; Li, J.-R.; Chang, H.-C.; Kitagawa, S.; Ribas, J. *Inorg. Chem.* **2005**, *44*, 9837. (d) Sloufova, I.; Sloufová, M. *Acta Crystallogr., Sect. C* **2000**, *56*, 1312. (e) Shakir, M.; Shahul Hameed, P.; Firdaus, F. *Synth. React. Inorg. Met.—Org. Chem.* **1994**, *24*, 1647. (f) Sabir, S.; Malik, A. U. *Synth. React. Inorg. Met.—Org. Chem.* **1994**, *24*, 1377. (g) Smith, T. J.; Walton, R. A. *Inorg. Nucl. Chem. Lett.* **1975**, *11*, 301. (h) Xiong, R.-G.; Zuo, J.-L.; You, X.-Z.; Fun, H.-K.; Raj, S. S. *Organometallics* **2000**, *19*, 1183. (i) Chen, Z. F.; Zhang, P.; Xiong, R. G.; Liu, D. J.; You, X. Z. *Inorg. Chem. Commun.* **2002**, *5*, 35.
- (6) For examples: (a) Ockwig, N. W.; Delgado-Friedrichs, O.; O'Keeffe, M.; Yaghi, O. M. *Acc. Chem. Res.* **2005**, *38*, 176. (b) Fujita, M.; Oka, H.; Yamaguchi, K.; Ogura, K. *Nature* **1995**, *378*, 469. (c) Losier, P.; Zaworotko, M. J. *Angew. Chem., Int. Ed.* **1996**, *35*, 2779. (d) Power, K. N.; Hennigar, T. L.; Zaworotko, M. J. *Chem. Commun.* **1998**, 595.
- (7) Alekseyeva, E. S.; Batsanov, A. S.; Boyd, L. A.; Fox, M. A.; Hibbert, T. G.; Howard, J. A. K.; MacBride, J. A. H.; Mackinnon, A.; Wade, K. J. *Chem. Soc., Dalton Trans.* **2003**, 475.
- (8) Juan, C. M. R.; Lee, B. *Coord. Chem. Rev.* **1999**, *183*, 43.
- (9) Guru Row, T. N. *Coord. Chem. Rev.* **1999**, *183*, 81.
- (10) Desiraju, G. R. *Acc. Chem. Res.* **1996**, *29*, 441.
- (11) Kuduva, S. S.; Craig, D. C.; Nangia, A.; Desiraju, G. R. *J. Am. Chem. Soc.* **1999**, *121*, 1936.

solid material structures, and many biological systems.^{15,16} Thus far, various C–H···M close interactions¹⁷ (M = Mo, Ti, Zr, Ru, Rh, Mn, Co, Cu, Fe, and Pd, etc.), such as the intermolecular multicenter heteroacceptor (IMH) hydrogen bonds and the intermolecular pseudoagostic (IPA) interactions,^{17a,b} have been studied and reported. However, reports on the supramolecular coordination systems containing C–H···Ag close interaction are still rare. To the best of our knowledge, only a few examples with C–H···Ag close interactions (either intermolecular or intramolecular) identified by X-ray diffraction on the basis of the van der Waals radii have been reported.¹⁸ Indeed, the intermolecular C–H···Ag close interactions are often much more important and frequent than intramolecular^{18d,e} in supramolecular coordination architectures. Moreover, reliable ways of pinning down these C–H···M close interactions are still at a premium, although examples containing various transition

- (12) Khlobystov, A. N.; Blake, A. J.; Champness, N. R.; Lemenovskii, D. A.; Majouga, A. G.; Zyk, N. V.; Schröder, M. *Coord. Chem. Rev.* **2001**, *222*, 155.
- (13) Unamuno, I.; Gutiérrez-Zorrilla, J. M.; Luque, A.; Román, P.; Lezama, L.; Calvo, R.; Rojo, T. *Inorg. Chem.* **1998**, *37*, 6452.
- (14) Tse, M. C.; Cheung, K. K.; Chan, M. C. W.; Che, C. M. *Chem. Commun.* **1998**, 2295.
- (15) For examples: (a) Lehn, J.-M. *Supramolecular Chemistry—Concepts and Perspectives*; VCH: Weinheim, Germany, 1995. (b) Desiraju, G. R. *Angew. Chem., Int. Ed.* **1995**, *34*, 2311. (c) Ye, B. H.; Tong, M. L.; Chen, X. M. *Coord. Chem. Rev.* **2005**, *249*, 545. (d) Wan, Y. H.; Zhang, L. P.; Jin, L. P.; Gao, S.; Lu, S. Z. *Inorg. Chem.* **2003**, *42*, 4985. (e) Sun, Z. M.; Mao, J. G.; Sun, Y. Q.; Zeng, H. Y.; Clearfield, A. *Inorg. Chem.* **2004**, *43*, 336. (f) Zheng, S. L.; Zhang, J. P.; Chen, X. M.; Huang, Z. L.; Lin, Z. Y.; Wong, W. T. *Chem.—Eur. J.* **2003**, *9*, 3888. (g) Whitesides, G. M.; Mathias, J. P.; Seto, C. T. *Science* **1991**, *254*, 1312.
- (16) For examples: (a) Fujita, M.; Ogura, K. *Coord. Chem. Rev.* **1996**, *148*, 249. (b) Kaes, C.; Katz, A.; Hosseini, M. W. *Chem. Rev.* **2000**, *100*, 3553. (c) Noro, S.; Kitaura, R.; Kondo, M.; Kitagawa, S.; Ishii, T.; Matsuzaka, H.; Yamashita, M. *J. Am. Chem. Soc.* **2002**, *124*, 2568. (d) Calhorda, M. J. *Chem. Commun.* **2000**, 801. (e) Hobza, P.; Havlas, Z. *Chem. Rev.* **2000**, *100*, 4253.
- (17) For examples: (a) Braga, D.; Greponi, F.; Tedesco, E.; Biradha, K.; Desiraju, G. R. *Organometallics* **1997**, *16*, 1846. (b) Thakur, T. S.; Desiraju, G. R. *Chem. Commun.* **2006**, 552. (c) Brookhart, M.; Green, M. L. H. *J. Organomet. Chem.* **1983**, *250*, 395. (d) Cotton, F. A.; LaCour, T.; Stanislawski, A. G. *J. Am. Chem. Soc.* **1974**, *96*, 754. (e) Scherer, W.; Hieringer, W.; Spiegler, M.; Sirsch, P.; McGrady, G. S.; Downs, A. J.; Haaland, A.; Pedersen, B. *Chem. Commun.* **1998**, 2471. (f) Pillet, S.; Wu, G.; Kulsomphob, V.; Harvey, B. G.; Ernst, R. D.; Coppens, P. *J. Am. Chem. Soc.* **2003**, *125*, 1937. (g) Yao, W. B.; Eisenstein, O.; Crabtree, R. H. *Inorg. Chim. Acta* **1997**, *254*, 105. (h) Corral, I.; Mó, O.; Yáñez, M. *Int. J. Mass Spectrom.* **2003**, *227*, 401. (i) Liu, C.-S.; Bu, X.-H. Unpublished work of the dinuclear Pd^{II} complex of L¹. (j) Brown, R. K.; Williams, J. M.; Schultz, A. J.; Stucky, G. D.; Ittel, S. D.; Harlow, R. L. *J. Am. Chem. Soc.* **1980**, *102*, 981. (k) Butts, M. D.; Bryan, J. C.; Luo, X.-L.; Kubas, G. *Inorg. Chem.* **1997**, *36*, 3341. (l) van der Boom, M. K.; Iron, M. A.; Atasoylu, O.; Simón, L. J. W.; Rozenberg, H.; Yehoshua, B. D.; Konstantinovskii, L.; Martinv, J. M. L.; Milstein, D. *Inorg. Chim. Acta* **2004**, *357*, 1854. (m) Patel, J.; Jackson, W. R.; Serelis, A. K. *Inorg. Chim. Acta* **2004**, *357*, 2374. (n) Kawamoto, T.; Nagasawa, I.; Kushi, Y.; Konno, T. *Inorg. Chim. Acta* **2003**, *348*, 217. (o) Siemer, C. J.; Meece, F. A.; Armstrong, W. H.; Eichhorn, D. M. *Polyhedron* **2001**, *20*, 2637. (p) Fang, X.; Huhmann-Vincent, J.; Scott, B. L.; Kubas, G. J. *J. Organomet. Chem.* **2000**, *609*, 95. (q) Castro, M.; Cruz, J.; Lopez-Sandoval, H.; Barba-Behrens, N. *Chem. Commun.* **2005**, 3779.
- (18) For examples: (a) McMorran, D. A. Steel, P. J. *Chem. Commun.* **2002**, 2120. (b) Steed, J. W.; Johnson, K.; Legido, C.; Junk, P. C. *Polyhedron* **2003**, *22*, 769 and references therein. (c) Sobocinski, R. L.; Pemberton, J. E. *Langmuir* **1992**, *8*, 2049. (d) Ingleson, M. J.; Mahon, M. F.; Patmore, N. J.; Ruggiero, G. D.; Weller, A. S. *Angew. Chem., Int. Ed.* **2002**, *41*, 3694. (e) Clarke, A. J.; Ingleson, M. J.; Kociok-Kohn, G.; Mahon, M. F.; Patmore, N. J.; Rourke, J. P.; Ruggiero, G. D.; Weller, A. S. *J. Am. Chem. Soc.* **2004**, *126*, 1503.

Chart 1



metals have been reported, as mentioned above,¹⁷ on the basis of structural or spectroscopic measurements or theoretical studies. Recently, Popelier^{19a} proposed an independent criterion for detecting and studying C–H···M close interaction by the Atoms in Molecules (AIM) theory that is different from some experimental criteria (XRD, NMR, and IR, etc.).^{19b} Several excellent reviews and papers have been published on this subject.²⁰

On the basis of all the aspects mentioned above, in this report, we have designed and prepared two structurally related rigid acridine-based ligands, 9-[3-(2-pyridyl)pyrazol-1-yl]acridine (**L**¹) and 9-(1-imidazolyl)acridine (**L**²) (Chart 1), and synthesized and characterized four of their Ag(I) complexes, {[AgL¹](ClO₄)₂}₂ (**1**), {[AgL¹](NO₃)₃}₂ (**2**), [AgL²](ClO₄) (**3**) and {[Ag₃L²](NO₃)₂(H₂O)}_∞ (**4**), by elemental analyses, IR spectroscopy, and single-crystal X-ray diffraction analysis, respectively. Interestingly, this work offers three new rare examples (**1**, **2**, and **4**) that exhibit C–H···Ag close interactions in which the N donors of the acridine rings coordinate to Ag(I) ions. From the viewpoint of geometrical requirements, the C–H···Ag weak interactions may have facilitated the formation of the coordination bond between Ag(I) and the N donor of the acridine ring. To compare with the experimental results of X-ray diffraction analysis, we have systematically carried out theoretical investigations of **1** by DFT calculations and AIM topological and NBO analyses, which give further confirmation and better understanding of the nature of C–H···Ag weak interactions and may offer us an effective means for constructing unique supramolecular architectures via C–H···M close interactions in coordination supramolecular systems.

Experimental Section

Materials and General Methods. 3-(2-Pyridyl)pyrazole was synthesized by reported procedures.²¹ All the other reagents for synthesis were commercially available and used as received or purified by standard methods prior to use. Melting points were measured on a X-4 micro melting point detector without further correction. Elemental analyses (C, H, N) were performed on a

Perkin–Elmer 240C analyzer and IR spectra on a Tensor 27 OPUS (Bruker) FT-IR spectrometer with KBr pellets. ¹H NMR spectra and 2D gCOSY spectrum were recorded on a Bruker AC-P500 spectrometer (300 MHz) at 25 °C in CDCl₃ (for **L**¹ and **L**²) and CD₃CN (for **L**¹, **L**², and **1–3**) with tetramethylsilane as the internal reference. The mass spectra were recorded on a Thermo Finnigan LCQ-Advantage spectrometer in ESI mode, I Spray Voltage 4.8 kV.

Synthesis of Ligands. **L**¹ and **L**² were synthesized according to modified literature procedures.²²

9-[3-(2-Pyridyl)pyrazol-1-yl]acridine (L**¹).** A mixture of 9-chloroacridine (5.5 mmol), 3-(2-pyridyl)-pyrazole (5.0 mmol), benzene (22 mL), ⁿBu₄NOH (0.25 mL, 40% aqueous solution), and aqueous NaOH (4.5 mL, 10 M) was heated at reflux for ca. 48 h with vigorous stirring. After the solution was cooled, the organic phase was separated, washed with H₂O, extracted with CHCl₃, collected, and dried over anhydrous MgSO₄. **L**¹ was obtained as light yellow powder and purified by recrystallization from CHCl₃/hexane (Yield: ~40% on the basis of 3-(2-pyridyl)-pyrazole). Mp: 150–152 °C. IR (KBr pellet, cm⁻¹): 3079m, 1629w, 1594m, 1557s, 1519m, 1489s, 1460m, 1439m, 1416s, 1370m, 1327w, 1283w, 1208w, 1153w, 1055w, 1042m, 992w, 960w, 910w, 812m, 759vs, 710w, 648m, 622w, 603w. ¹H NMR (300 MHz, CDCl₃, 25 °C, TMS): δ 7.314–7.338 (m, 1H), 7.487 (d, *J* = 3.6 Hz, 1H), 7.576–7.628 (m, 2H), 7.793 (d, *J* = 7.5 Hz, 3H), 7.859–7.907 (m, 2H), 7.963 (d, *J* = 2.4 Hz, 1H), 8.148 (d, *J* = 8.1 Hz, 1H), 8.428 (d, *J* = 7.5 Hz, 2H), 8.742 (d, *J* = 4.2 Hz, 1H). ¹H NMR (300 MHz, CD₃CN, 25 °C, TMS): δ 7.358–7.404 (m, 2H), 7.623–7.674 (m, 2H), 7.727–7.750 (m, 2H), 7.825–7.951 (m, 3H), 8.064 (d, *J* = 7.622 Hz, 1H), 8.141 (d, *J* = 2.345 Hz, 1H), 8.312 (d, *J* = 8.795 Hz, 2H), 8.675 (d, *J* = 4.691 Hz, 1H). Anal. Found: C, 77.81; H, 4.84; N, 16.95. Calcd for C₂₁H₁₄N₄: C, 78.24; H, 4.38; N, 17.38.

9-(1-Imidazolyl)acridine (L**²).** **L**² was obtained as a yellow powder in ~50% yield in a similar procedure. Mp: 210–213 °C. IR (KBr pellet, cm⁻¹): 3064w, 1624w, 1667m, 1543m, 1513m, 1458m, 1432m, 1392s, 1313m, 1273s, 1146m, 1009w, 943s, 847w, 820s, 773br, 758vs, 642m, 599m, 589m, 567m. ¹H NMR (300 MHz, CDCl₃, 25 °C, TMS): δ 7.383 (s, 1H), 7.514 (s, 1H), 7.612 (d, *J* = 3.0 Hz, 4H), 7.858–7.900 (m, 3H), 8.379 (d, *J* = 5.4 Hz, 2H). ¹H NMR (300 MHz, CD₃CN, 25 °C, TMS): δ 7.414 (s, 1H), 7.524 (s, 1H), 7.577 (d, *J* = 8.795 Hz, 2H), 7.643–7.694 (m, 2H), 7.901–7.952 (m, 3H), 8.298 (d, *J* = 8.795 Hz, 2H). Anal. Found: C, 77.98; H, 4.95; N, 16.81. Calcd for C₁₆H₁₁N₃: C, 78.35; H, 4.52; N, 17.13.

Synthesis of Complexes. Yellow single crystals of **1–4** suitable for X-ray analysis were obtained by a method similar to that described below for **1**.

{[AgL¹](ClO₄)₂}₂ (**1**). A solution of AgClO₄·H₂O (0.1 mmol) in CH₃OH (15 mL) was carefully layered on top of a CHCl₃ solution (10 mL) of **L**¹ (0.05 mmol) in a test tube. Yellow single crystals suitable for X-ray analysis appeared at the boundary between CH₃OH and CHCl₃ after ca. two weeks at room temperature. Yield: ~50%. Anal. Calcd for C₂₁H₁₄AgCl₂N₄O₈: C, 47.62; H, 2.66; N, 10.58. Found: C, 47.23; H, 2.48; N, 10.09. IR (KBr, cm⁻¹): 3099w, 1627w, 1608m, 1497m, 1424s, 1387w, 1372m, 1289w, 1161w, 1095vs, 1023m, 960w, 913w, 826w, 781m, 760vs, 710w, 653m, 622s, 604m, 510w. ¹H NMR (300 MHz, CD₃CN, 25 °C, TMS): δ 7.227–7.268 (m, 2H), 7.305 (d, *J* = 2.345 Hz, 2H), 7.494–7.568

(19) For examples: (a) Popelier, P. L. A.; Logothetis, G. J. *Organomet. Chem.* **1998**, 555, 101. (b) Elschenbroich, C.; Salzer, A. *Organometallics: A Concise Introduction*; VCH: Weinheim, Germany, 1992. (20) For examples: (a) Bader, R. F. W. *Atoms in Molecules: A Quantum Theory*; Clarendon Press: Oxford, U.K., 1990. (b) Koritsansky, T. S.; Coppens, P. *Chem. Rev.* **2001**, 101, 1583. (c) Bader, R. F. W. *Chem. Rev.* **1991**, 91, 893. (d) Matta, C. F.; Hernández-Trujillo, J.; Tang, T.-H.; Bader, R. F. W. *Chem.–Eur. J.* **2003**, 9, 1940. (e) Fang, D.-C.; Tang, T.-H. *AIM98PC* (modified PC version of AIM98PC).

(21) For examples: (a) Brunner, H.; Scheck, T. *Chem. Ber.* **1992**, 125, 701. (b) Lin, Y.; Lang, S. A. *J. Heterocycl. Chem.* **1977**, 14, 345.

(22) For examples: (a) Ward, M. D.; McCleverty, J. A.; Jeffery, J. C. *Coord. Chem. Rev.* **2001**, 222, 251. (b) Zhang, H.; Liu, C.-S.; Bu, X.-H.; Yang, M. J. *Inorg. Biochem.* **2005**, 99, 1119 and references therein.

Table 1. Crystallographic Data and Structure Refinement Summary for Complexes 1–4

	1	2	3	4
chemical formula	C ₂₁ H ₁₄ AgClN ₄ O ₄	C ₂₁ H ₁₄ AgN ₅ O ₃	C ₃₂ H ₂₂ AgClN ₆ O ₄	C ₄₈ H ₃₅ Ag ₃ N ₁₂ O ₁₀
fw	529.68	492.24	697.88	1263.49
cryst syst	monoclinic	triclinic	monoclinic	monoclinic
space group	<i>P</i> 2(1)/ <i>c</i>	<i>P</i> 1	<i>C</i> 2/ <i>c</i>	<i>P</i> 2(1)/ <i>c</i>
<i>a</i> (Å)	6.905(4)	9.178(3)	26.354(9)	13.2563(2)
<i>b</i> (Å)	15.537(8)	9.271(3)	8.442(3)	20.4398(4)
<i>c</i> (Å)	18.622(10)	12.292(4)	14.618(5)	17.2388(3)
α (deg)	90	68.588(5)	90	90
β (deg)	96.413(9)	75.457(5)	117.527(5)	107.2350(10)
γ (deg)	90	72.949(5)	90	90
<i>V</i> (Å ³)	1985.2(19)	918.7(5)	2884.1(16)	4461.22(13)
<i>Z</i>	4	2	4	4
<i>D</i> (g cm ⁻³)	1.772	1.779	1.607	1.881
μ (mm ⁻¹)	1.188	1.133	0.841	1.382
GOF	1.014	1.000	0.919	1.079
<i>T</i> (K)	293(2)	293(2)	293(2)	293(2)
<i>R</i> ^a / <i>wR</i> ^b	0.0355/0.0822	0.0478/0.0823	0.0470/0.0926	0.0295/0.0784

$$^a R = \sum(|F_o| - |F_c|) / \sum|F_o|. \quad ^b wR = [\sum w(|F_o|^2 - |F_c|^2) / \sum w(F_o^2)]^{1/2}.$$

(m, 8H), 7.760–7.817 (m, 4H), 7.842–7.895 (m, 2H), 7.952 (d, *J* = 7.622 Hz, 2H), 8.116 (s, 2H), 8.138 (d, *J* = 2.345 Hz, 4H), 8.192 (d, *J* = 4.691 Hz, 2H). MS (ESI): *m/z* 429.36 for [Ag₂(L¹)₂]²⁺.

{[AgL¹](NO₃)₂ (2)}. Yield: ~40%. Anal. Calcd for C₂₁H₁₄AgN₅O₃: C, 51.24; H, 2.87; N, 14.23. Found: C, 50.78; H, 2.53; N, 14.55. IR (KBr, cm⁻¹): 3094w, 1597m, 1559s, 1519s, 1494m, 1425vs, 1315vs, 1097w, 1061m, 1015m, 960m, 824w, 783m, 759vs, 651m, 604s. ¹H NMR (300 MHz, CD₃CN, 25 °C, TMS): δ 7.291–7.346 (m, 4H), 7.584–7.683 (m, 8H), 7.832–7.915 (m, 6H), 8.002 (d, *J* = 8.208 Hz, 2H), 8.147 (d, *J* = 2.345 Hz, 2H), 8.262 (d, *J* = 8.795 Hz, 4H), 8.424 (d, *J* = 4.104 Hz, 2H). MS (ESI): *m/z* 429.37 for [Ag₂(L¹)₂]²⁺.

[AgL²](ClO₄) (3). Yield: ~50%. Anal. Calcd for C₃₂H₂₂AgClN₆O₄: C, 55.07; H, 3.18; N, 12.04. Found: C, 54.71; H, 2.71; N, 11.72. IR (KBr, cm⁻¹): 3121w, 1629w, 1613w, 1553w, 1508s, 1465m, 1439w, 1423w, 1363w, 1324m, 1265w, 1227w, 1101vs, 1037br, 949w, 857w, 797w, 757vs, 660m, 642w, 621w, 601s, 422w. ¹H NMR (300 MHz, CD₃CN, 25 °C, TMS): δ 7.424 (d, *J* = 1.173 Hz, 2H), 7.541–7.586 (m, 6H), 7.645–7.692 (m, 4H), 7.901–7.969 (m, 6H), 8.301 (d, *J* = 8.795 Hz, 4H). MS (ESI): *m/z* 597.22 for [Ag(L²)₂]⁺.

{[(Ag₃L²)(NO₃)](NO₃)₂(H₂O)}_∞ (4). Yield: ~40%. Anal. Calcd for C₄₈H₃₅Ag₃N₁₂O₁₀: C, 45.63; H, 2.79; N, 13.30. Found: C, 46.03; H, 2.33; N, 13.61. IR (KBr, cm⁻¹): 3102w, 1629m, 1603m, 1554s, 1490vs, 1320vs, 1150w, 1111m, 1088s, 1032s, 933w, 858m, 797w, 754vs, 659s, 601m.

Caution! Although we have met no problems in handling perchlorate salts during this work, these should be treated cautiously because of their potential explosive nature.

X-ray Data Collection and Structure Determinations. X-ray single-crystal diffraction data for complexes 1–4 were collected on a Bruker Smart 1000 CCD diffractometer at 293(2) K with Mo K α radiation (λ = 0.71073 Å) by the ω scan mode. The program SAINT²³ was used for integration of the diffraction profiles. All the structures were solved by direct methods using the SHELXS program of the SHELXTL package and refined by full-matrix least-squares methods with SHELXL (semiempirical absorption corrections were applied using SADABS program).²⁴ Metal atoms in each complex were located from the *E*-maps and other non-hydrogen atoms were located in successive difference Fourier syntheses and refined with anisotropic thermal parameters on *F*². The hydrogen

atoms of the ligands were generated theoretically onto the specific atoms and refined isotropically with fixed thermal factors. Further details for structural analysis are summarized in Table 1.

Calculation Details. The DFT calculations were performed using the Gaussian 03 suite of programs on a DeepComp 6800 supercomputer at the Chinese Academy of Science and a Nankai Stars supercomputer at Nankai University.²⁵ A combination of Becke's three-parameter hybrid function with Lee–Yang–Parr's exchange function was applied for 1 as the representative complex and free ligand L¹ for comparison.²⁶ The Ag(I) ions in 1 have been described with the LANL2DZ basis set, including effective core potentials, whereas the 6-31++G** basis set has been used for C, N, O, and H atoms. The geometries of complex 1 and free ligand L¹, on the basis of the crystal structure, were fully optimized. Meanwhile, the vibrational frequency calculations were carried out to ensure that the stationary points located on the potential energy surfaces by geometry optimization were minima. Also, the electron density and charge distribution have been investigated using NBO analysis. In addition, on the basis of the wave functions obtained from the geometry optimization of 1, the topological properties (electron densities ρ_b and Laplacians $\nabla^2\rho_b$ at bond critical points (BCPs) and electron densities ρ_r and Laplacians $\nabla^2\rho_r$ at ring critical points (RCPs)), maps of the charge density distributions, and Laplacian

(24) (a) Sheldrick, G. M. *SHELXTL NT: Program for Solution and Refinement of Crystal Structures*, version 5.1; University of Göttingen, Germany, 1997. (b) Sheldrick, G. M. *SADABS, Siemens Area Detector Absorption Corrected Software*; University of Göttingen: Göttingen, Germany, 1996.

(25) Frisch, M. J.; Trucks, G. W.; Schlegel, H. B.; Scuseria, G. E.; Robb, M. A.; Cheeseman, J. R.; Montgomery, J. A.; Vreven, T., Jr.; Kudin, K. N.; Burant, J. C.; Millam, J. M.; Iyengar, S. S.; Tomasi, J.; Barone, V.; Mennucci, B.; Cossi, M.; Scalmani, G.; Rega, N.; Petersson, G. A.; Nakatsuji, H.; Hada, M.; Ehara, M.; Toyota, K.; Fukuda, R.; Hasegawa, J.; Ishida, M.; Nakajima, T.; Honda, Y.; Kitao, O.; Nakai, H.; Klene, M.; Li, X.; Knox, J. E.; Hratchian, H. P.; Cross, J. B.; Adamo, C.; Jaramillo, J.; Gomperts, R.; Stratmann, R. E.; Yazyev, O.; Austin, A. J.; Cammi, R.; Pomelli, C.; Ochterski, J. W.; Ayala, P. Y.; Morokuma, K.; Voth, G. A.; Salvador, P.; Dannenberg, J. J.; Zakrzewski, V. G.; Dapprich, S.; Daniels, A. D.; Strain, M. C.; Farkas, O. D.; Malick, K.; Rabuck, A. D.; Raghavachari, K.; Foresman, J. B.; Ortiz, J. V.; Cui, Q.; Baboul, A. G.; Clifford, S.; Cioslowski, J.; Stefanov, B. B.; Liu, G.; Liashenko, A.; Piskorz, P.; Komaromi, I.; Martin, R. L.; Fox, D. J.; Keith, T.; Al-Laham, M. A.; Peng, C. Y.; Nanayakkara, A.; Challacombe, M.; Gill, P. M. W.; Johnson, B.; Chen, W.; Wong, M. W.; Gonzalez, C.; Pople, J. A. *Gaussian 03*, revision C.01; Gaussian, Inc.: Pittsburgh, PA, 2003.

(26) Becke, A. D. *J. Chem. Phys.* **1993**, *98*, 5648. (b) Lee, C.; Yang, W.; Parr, R. G. *Phys. Rev. B* **1988**, *37*, 785.

(23) *SAINT Software Reference Manual*; Bruker AXS: Madison, WI, 1998.

distributions were investigated with the program AIM98PC, which was modified by Fang et al. from the AIMPAC package.^{20e}

Results and Discussion

Synthesis Consideration and General Characterization.

Both ligands **L**¹ and **L**² are soluble in most common polar organic solvents (such as CH₂Cl₂, CHCl₃, CH₃OH, and CH₃CN), so that crystallization of their complexes with inorganic metal salts occurs readily. Complexes **1–4** were obtained as crystalline compounds in a CH₃OH/CHCl₃ mixed-solvent system by combining the corresponding ligands with different Ag(I) salts by diffusion. **1–4** are air stable at room temperature. To further investigate the behavior in solution of **1–3** (three multinuclear discrete complexes), we have recorded their mass spectra in ESI mode. The result demonstrates that **1–3** are stable in acetonitrile solutions and appear to exist as discrete [Ag₂(L¹)₂]²⁺ species (**1** and **2**) and [Ag(L²)₂]⁺ species (**3**), respectively (found *m/z* 429.36 for **1**, 429.37 for **2**, and 597.22 for **3**; calcd *m/z* 429.02 for **1**, 429.02 for **2**, and 597.10 for **3**, see the Supporting Information, Figures S7–S9). In addition, in comparison with the free ligands **L**¹ and **L**², the ¹H NMR spectra of **1–3** are also consistent with their monomeric structures and the signals for the protons are obviously shifted upfield by ca. 0.1–0.2 ppm (see the Supporting Information, Figures S1–S6). As a typical example, upon coordination to silver(I), the signals for H(4A) and H(5A) of the **L**¹ ligand in **1** are shifted upfield by an average of ca. 0.17 ppm (see the Supporting Information, Figures S1–S3). Complete assignment of the ¹H NMR spectrum for **L**¹ was further achieved by a 2D gCOSY experiment (see the Supporting Information, Figure S2).

Descriptions of Crystal Structures for 1–4. {[AgL¹](ClO₄)₂ (**1**). The structure of **1** consists of a dinuclear [Ag₂(L¹)₂]²⁺ unit and two uncoordinated ClO₄⁻ compounds. The dinuclear [Ag₂(L¹)₂]²⁺ cation (Figure 1a) comprises two **L**¹ and two Ag(I) ions; each Ag(I) takes a distorted trigonal planar geometry formed by three N donors, two from the pyridyl–pyrazole ring of **L**¹ and one from the acridine ring of another **L**¹. The bond distances and angles around each Ag(I) center are within the normal range expected for such coordination complexes (Table 2).²⁷ Moreover, in the dinuclear subunit of **1**, the centroid–centroid separation between two parallel neighboring acridine rings is 3.681 Å, the dihedral angle between them is 2.0°, and the average interplanar separation is 3.495 Å, indicating the existence of significantly intramolecular face-to-face π···π stacking interactions.²⁸ Also, it is worth noting that examination of the intramolecular distances further shows the presence of obvious C–H···M close intramolecular interactions between

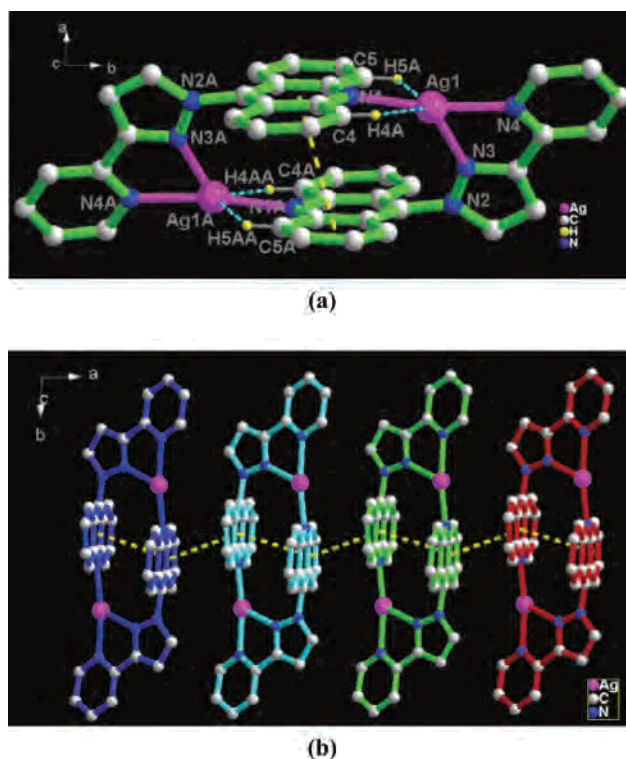


Figure 1. View of (a) the coordination environment of Ag(I) with intramolecular C–H···Ag H-bonding and face-to-face π···π stacking interactions and (b) the 1D chain linked by the intermolecular π···π stacking interaction in **1** (H atoms and uncoordinated ClO₄⁻ omitted for clarity).

Table 2. Selected Bond Distances (Å) and Angles (deg) for Complexes **1–4**^a

Complex 1			
Ag(1)–N(1)	2.177(3)	Ag(1)–N(4)	2.219(3)
Ag(1)–N(3)	2.418(3)		
N(1)–Ag(1)–N(4)	171.52(9)	N(1)–Ag(1)–N(3)	114.73(8)
N(4)–Ag(1)–N(3)	71.93(9)		
Complex 2			
Ag(1)–N(4)	2.266(3)	Ag(1)–N(3)	2.340(3)
Ag(1)–N(2)	2.457(3)		
N(4)–Ag(1)–N(3)	158.84(12)	N(4)–Ag(1)–N(2)	110.52(11)
N(3)–Ag(1)–N(2)	69.36(12)		
Complex 3			
Ag(1)–N(1)	2.085(3)	Ag(1)–N(1A)	2.085(3)
N(1A)–Ag(1)–N(1)	180.00(18)		
Complex 4			
Ag(1)–N(6)	2.169(2)	Ag(1)–N(1)	2.212(2)
Ag(2)–N(3)	2.141(2)	Ag(2)–N(4)	2.179(2)
Ag(2)–O(6)	2.598(2)	Ag(3)–N(7B)	2.112(2)
Ag(3)–N(9)	2.162(2)		
N(6)–Ag(1)–N(1)	166.37(9)	N(3)–Ag(2)–N(4)	168.27(8)
N(3)–Ag(2)–O(6)	86.46(8)	N(4)–Ag(2)–O(6)	104.28(8)
N(7B)–Ag(3)–N(9)	171.15(8)		

^a Symmetry codes for **3** and **4**: A $-x, -y + 1, -z + 1$; B $-x + 1/2, y + 1/2, -z + 1/2$.

the Ag centers and the acridine ring H(4A) and H(5A) atoms, with Ag···H distances of 2.657–2.706 Å, Ag···C distances of 3.198–3.231 Å ($d(\text{Ag}\cdots\text{H}) < d(\text{Ag}\cdots\text{C})$), and C–H···Ag angles of 116.60–117.73° (C–H···Ag > 100°) (see Table 3), which, to the best of our knowledge, are similar to those values for reported Ag(I)–acridine complexes.^{5d} Therefore, such C–H···M close interaction mentioned above

- (27) For examples: (a) Orpen, A. G.; Brammer, L.; Aleen, F. H.; Kennard, O.; Watson, D. G.; Taylor, R. *J. Chem. Soc., Dalton Trans.* **1989**, S1. (b) Aleen, F. H.; Kennard, O.; Watson, D. G.; Brammer, L.; Orpen, A. G.; Taylor, R. *J. Chem. Soc., Perkin Trans. II* **1987**, S1. (c) O’Keeffe, M.; Brese, N. E. *J. Am. Chem. Soc.* **1991**, *113*, 3226. (28) For examples: (a) Janiak, C. *J. Chem. Soc., Dalton Trans.* **2000**, 3885. (b) Zou, R. Q.; Liu, C. S.; Huang, Z.; Hu, T. L.; Bu, X. H. *Cryst. Growth Des.* **2006**, *6*, 99. (c) Bu, X. H.; Xie, Y. B.; Li, J. R.; Zhang, R. H. *Inorg. Chem.* **2003**, *23*, 7422.

Table 3. C–H···Ag Hydrogen-Bonding Geometry (Å, deg) for **1**, **2**, and **4**

C–H···Ag	C–H	H···Ag	C···Ag	C–H···Ag
1				
C(4)–H(4A)···Ag(1)	0.930	2.706	3.231	116.60
C(5)–H(5A)···Ag(1)	0.931	2.657	3.198	117.73
2				
C(9)–H(9A)···Ag(1)	0.930	2.776	3.317	118.09
C(16)–H(16A)···Ag(1)	0.930	2.673	3.234	119.45
4				
C(2)–H(2A)···Ag(1)	0.931	2.689	3.239	118.61
C(2)–H(12A)···Ag(1)	0.931	2.689	3.235	118.27
C(18)–H(18A)···Ag(2)	0.930	2.702	3.235	117.27
C(18)–H(28A)···Ag(2)	0.930	2.620	3.168	118.22
C(28)–H(34A)···Ag(3)	0.929	2.731	3.255	116.56
C(28)–H(44A)···Ag(3)	0.931	2.585	3.132	118.03

should be well-described as being weak intramolecular C–H···M hydrogen bonding (a special case of hydrogen bonding); this depiction is also chemically and geometrically more reasonable.^{17a,b,18} Moreover, from the viewpoint of geometrical requirements, the C–H···Ag weak interactions may have facilitated the formation of the coordination bond between Ag(I) and the N donor of the acridine ring in the solid state.

In addition, the centroid–centroid separation between the intermolecular adjacent acridine rings is 3.654 Å, and then the intra- and intermolecular face-to-face π ··· π stacking interactions link the dinuclear cations into a quasi-1D chain (Figure 1b).²⁸

{[AgL¹](NO₃)₂}₂ (**2**). The reaction of L¹ with AgNO₃ instead of AgClO₄·H₂O, similar to **1**, also gave a dinuclear complex, **2**, consisting of a centrosymmetric [Ag₂(L¹)₂]²⁺ cation and two uncoordinated NO₃[−] anions (Figure 2a). All the Ag–N bond distances and bond angles around each Ag(I) center are in the normal range for such complexes (2.266–(3)–2.457(3) Å and 69.36(1)–158.84(1)°; Table 2).²⁷ The centroid–centroid separation of 3.580 Å, dihedral angle of 1.3°, and average interplanar separation of 3.434 Å between acridine rings in the dinuclear unit indicate a significant intramolecular face-to-face π ··· π stacking interaction.²⁸ Moreover, similar to **1**, the Ag···H distances of 2.673–2.776 Å, Ag···C distances of 3.234–3.317 Å ($d(\text{Ag}\cdots\text{H}) < d(\text{Ag}\cdots\text{C})$) and C–H···Ag angles of 118.09–119.45° (C–H···Ag > 100°) between the Ag(I) centers and the acridine ring H9A and H16A hydrogens also exhibit the presence of C–H···M weak interactions (see Table 3).^{17a,b,18} Different from **1**, however, each uncoordinated NO₃[−] shows an obvious Ag···O weak interaction with the Ag(I) center of one dinuclear unit (the Ag···O distances are ca. 2.706 and 2.704 Å). Therefore, the co-effects of the intramolecular π ··· π stacking and C–H···Ag and Ag···O weak interactions mentioned above further help to stabilize the dinuclear structure of **2** in the solid state.

Different from **1**, in **2**, the adjacent discrete dinuclear units are arranged into a quasi-1D chain not by π ··· π stacking interaction but by the weak intermolecular C–H···O hydrogen-bonding interaction between the uncoordinated O-atoms of NO₃[−] anions and H atoms of pyrazole rings. The C(1)···

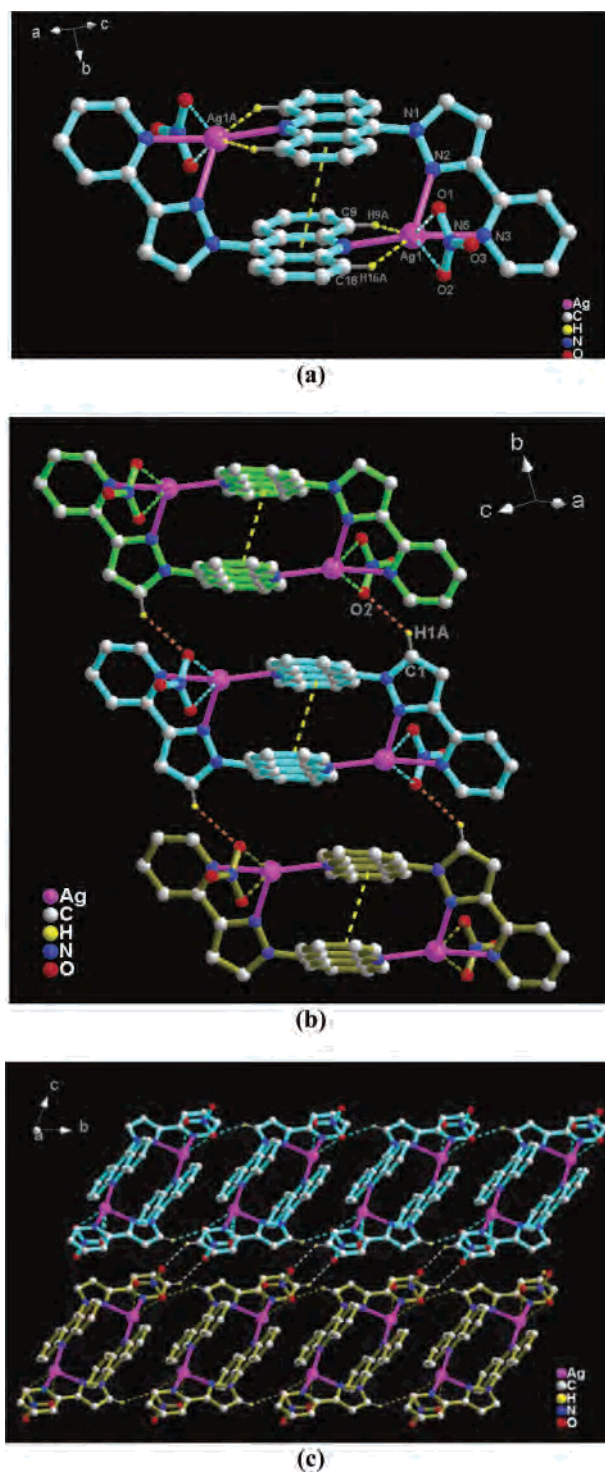


Figure 2. View of (a) the coordination environment of Ag(I) with intramolecular C–H···Ag H-bonding, face-to-face π ··· π stacking, and Ag···O interactions; (b) the 1D chain linked by the intermolecular π ··· π stacking and the C–H···O H-bonding interactions; and (c) the 2D network formed through interchain C–H···O H-bonding interaction in **2** (H atoms omitted for clarity).

O(2)#1 separation is 3.2071 Å with a C(1)–H(1A)···O(2)-#1 angle of 141.4(3)° (#1 = 1 – x, 1 – y, 1 – z; Figure 2b). In addition, the adjacent 1D chains are further linked to form a quasi-2D network through the intermolecular weak C–H···O hydrogen-bonding interaction (C(7)–H(7A)···O(3)#2, #2 = x, –1 + y, z) with a separation of 3.273(1) Å

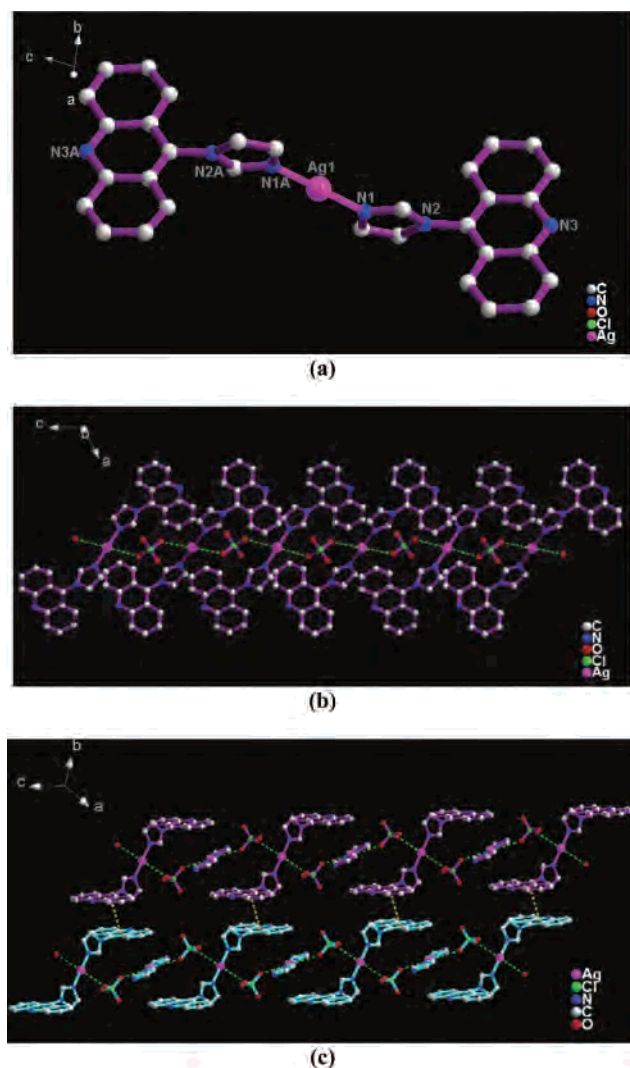


Figure 3. View of (a) the coordination environment of Ag(I), (b) the 1D chain linked by the intermolecular Ag \cdots O interactions, and (c) the 2D network formed through interchain face-to-face $\pi\cdots\pi$ stacking interactions in **3** (H atoms omitted for clarity).

for C(7) \cdots O(3)#2 and an angle of 133.8(4) $^\circ$ for C(7)–H(7A) \cdots O(3)#2 (Figure 2c).²⁹

[AgL₂](ClO₄) (3). The crystal structure of **3** consists of discrete [AgL₂]⁺ and ClO₄[−]. The perspective view of the mononuclear entity in **3** with atomic labeling is given in Figure 3a with uncoordinated ClO₄[−] and H atoms omitted for clarity; the selected bond lengths and angles are listed in Table 2. Each Ag(I) center adopts a linear coordination geometry coordinated by two imidazole N donors from two distinct L² ligands. The Ag–N bond distances fall in the expected range for such coordination bonds (2.085(3) Å), and the N–Ag–N angles (180 $^\circ$) are close to those of two coordinated Ag(I) complexes (172–180 $^\circ$).²⁷ On the other hand, the L² ligand coordinates to the Ag(I) center not in an *N,N*-bidentate bridging mode but in an *N*-monodentate coordination mode with one N donor of the imidazole ring,

(29) For examples: (a) Desiraju, G. R.; Steiner, T. *The Weak Hydrogen Bond in Structural Chemistry and Biology*; Oxford University Press: Oxford, U.K., 1999. (b) Zou, R. Q.; Bu, X. H.; Zhang, R. H. *Inorg. Chem.* **2004**, *43*, 5382. (c) Barberà, G.; Viñas, C.; Teixidor, F.; Rosair, G. M.; Welch, A. J. *J. Chem. Soc., Dalton Trans.* **2002**, 3647.

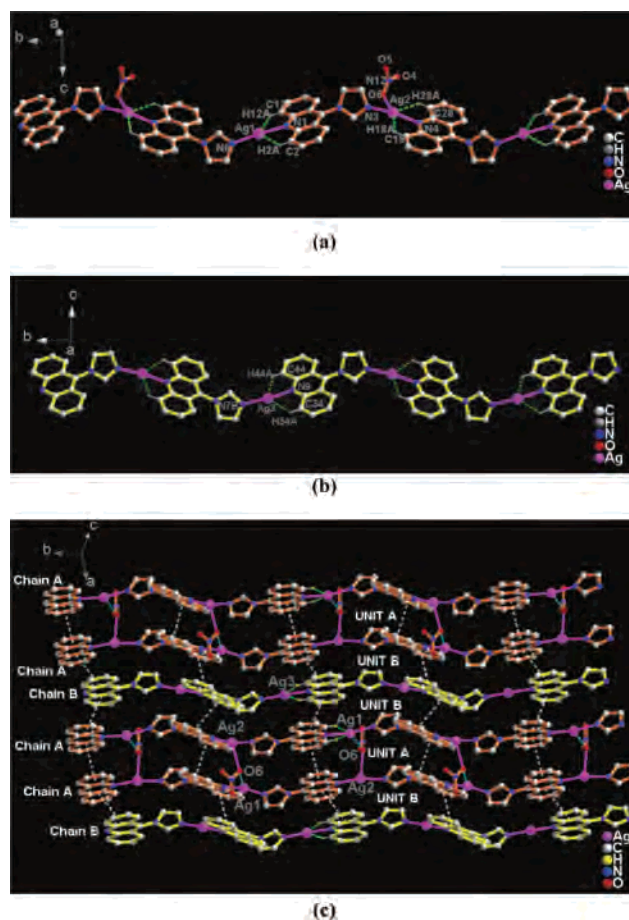


Figure 4. View of (a) the coordination environment of Ag(I) in Chain A with the intrachain C–H \cdots Ag H-bonding interactions, (b) the coordination environment of Ag(I) in Chain B with the intrachain C–H \cdots Ag H-bonding interactions, and (c) the 2D network formed through interchain $\pi\cdots\pi$ stacking and Ag \cdots O interactions in **4** (H atoms and uncoordinated NO₃[−] anions omitted for clarity).

namely, the N donor of the acridine ring, not joining the coordination geometry, thus resulting in a mononuclear entity instead of an infinite structure like that in **4**, which will be discussed later.

Another feature of **3** is the formation of a quasi-1D chain by Ag \cdots O weak interaction (the Ag \cdots O distance is ca. 3.262 Å) between Ag(I) centers and uncoordinated ClO₄[−] anions (Figure 3b). In addition, there were obvious interchain face-to-face $\pi\cdots\pi$ stacking interactions between the acridine rings of adjacent chains with a centroid–centroid separation of 3.629 Å, dihedral angle of 0.6 $^\circ$, and average interplanar separation of 3.5847 Å. Such a type of intermolecular face-to-face $\pi\cdots\pi$ stacking interaction links the 1D chains into the quasi-2D supramolecular network, which further enhances the stability of **3** in the solid state (Figure 3c).²⁸

{[Ag₃L₃](NO₃)](NO₃)₂(H₂O)} ∞ (4). Different from **3**, the structure of **4** has a more complicated and interesting framework consisting of stacks of two different 1D coordination motifs (defined as units A, units B, chains A, and chains B, Figure 4). In **4**, each L² ligand takes a bidentate bridging coordination fashion and links two Ag(I) centers with two N donors from imidazole and acridine rings of L² to form a nearly linear chain. Unit A is made of two equivalent and almost parallel 1D cationic A chains. In chain A, there are

two different Ag(I) centers (Ag(1) and Ag(2)) in an asymmetric unit. Ag(1) adopts a linear coordination geometry coordinated by two N donors of imidazole and acridine ring from two distinct L^2 ligands, and Ag(2) has a slightly distorted T-shaped geometry coordinated by an imidazole N donor, an acridine N donor from different L^2 ligands, and an O donor from NO_3^- (Figure 4a). On the other hand, in chain **B**, each Ag(I) is in only a linear coordination environment and binds to two N donors of imidazole and acridine from two distinct L^2 ligands (Figure 4b). In the ladderlike structure of unit **A**, the separations of $Ag\cdots Ag$ across the NO_3^- anion and L^2 are 4.878 and 10.404 Å, respectively. Two adjacent **A** chains are related by an inversion center and are offset by a ligand interval with each other along the direction in which the ladderlike structure of **A** units propagates. Similar to that in **1** and **2**, it should be pointed out that **4** also shows the existence of surprisingly weak C–H···Ag interactions, with $Ag\cdots H$ distances of 2.585–2.731 Å, $Ag\cdots C$ distances of 3.132–3.255 Å ($d(Ag\cdots H) < d(Ag\cdots C)$), and C–H···Ag angles of 116.56–118.61° (C–H···Ag > 100°) (see Table 3).^{17a,b,18}

In addition to coordinating to Ag(2) centers, O(6) atoms of coordinated NO_3^- in the cavities of **A** units also show weak $Ag\cdots O$ interaction with Ag(1) of the other **A** chain (the $Ag\cdots O$ distance is ca. 2.703(2) Å) to link two **A** chains into the ladderlike structure of **A** units. Meanwhile, the strong face-to-face $\pi\cdots\pi$ stacking interaction of **A** chains in **A** units is observed, with centroid–centroid separations of 3.467 and 3.553 Å. Also, in **B** units, there are weak $\pi\cdots\pi$ stacking interactions between **A** units and **B** chains (the centroid–centroid separations are 3.712 and 3.805 Å, respectively).²⁸ These weak interactions contribute greatly to the linkage of **A** chains, **B** chains, **A** units, and **B** units, forming the 2D supramolecular network (Figure 4c).

Theoretical Computational Results

To further confirm and better understand the presence and nature of the C–H···Ag hydrogen-bonding interactions, we carried out full geometry optimization on the basis of the experimental structure, the natural bond orbital (NBO),³⁰ and topological analysis of **1**, as a representative example, by DFT and AIM²⁰ calculations.³¹ The superimposed structures were obtained after a LSQ fitting of the optimized geometry and the experimental structure (Figure 5); the root-mean-square deviation (RMSD) of the two structures is 0.571 Å, indicating that the optimized geometry is generally in good agreement with the experimental results. The slight discrepancies are probably a consequence of crystal-packing forces and the presence of the counteranions in the solid-state structure (Table 4).

Several studies on H-bonded and C–H···M systems have pointed out that the formation of hydrogen bonds is always associated with the appearance of bond critical points (BCPs)

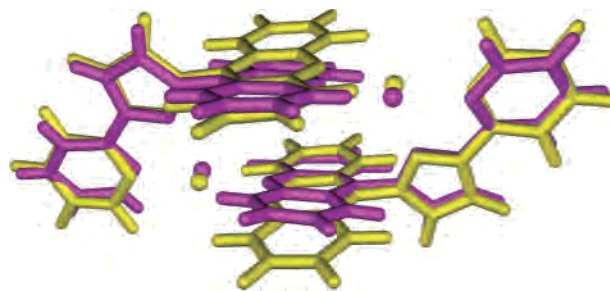


Figure 5. View of the superimposed structures on the basis of the experimental structure and the optimized geometry of **1** (the purple one is the experimental structure and the yellow is the optimized geometry).

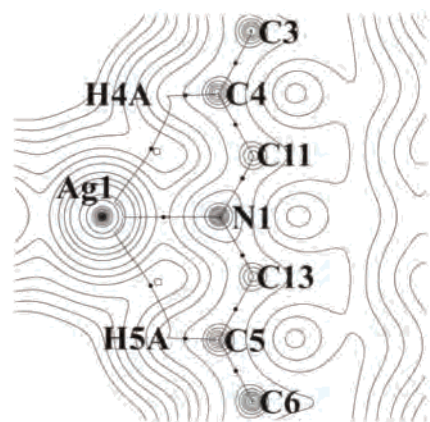
Table 4. Selected Geometric Parameters of the Crystal Structure and Calculated Geometry (the corresponding geometric parameters in the isolated free ligand L^1 are given in parentheses)

	crystal structure	computed geometry
$d_{Ag(1)-N(1)}$	2.177	2.241
$d_{Ag(1)-N(2)}$	3.575	3.682
$d_{Ag(1)-N(3)}$	2.418	2.509
$d_{Ag(1)-N(4)}$	2.219	2.270
$d_{Ag(1)\cdots C(4)}$	3.232	3.277
$d_{Ag(1)\cdots C(5)}$	3.198	3.272
$d_{C(4)-H(4A)}$	0.930	1.087 (1.085)
$d_{C(5)-H(5A)}$	0.930	1.087 (1.085)
$\theta_{N(3)-C(16)-C(17)-N(4)}$	10.615	-3.325 (-23.84)
$\theta_{N(3A)-N(2A)-C(9)-C(10)}$	-114.685	-97.852 (-117.55)

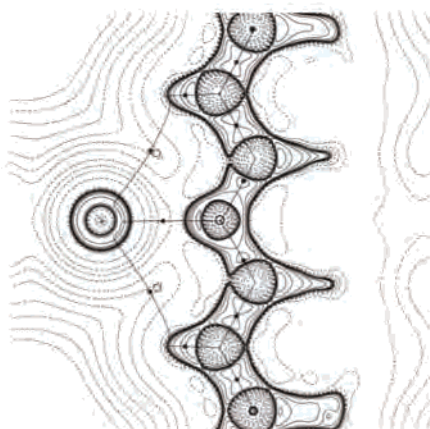
between the H and acceptor atoms,^{19,20} which are often linked by concomitant bond paths. The (3, -1) BCPs ($\rho_b = 0.0110$ e au⁻³, $\nabla^2\rho_b = 0.0386$ e au⁻⁵ and $\rho_b = 0.0112$ e au⁻³, $\nabla^2\rho_b = 0.0391$ e au⁻⁵) between Ag(1) and H(4A)/H(5A) were found to be 1.636/1.630 Å away from Ag(1), suggesting that the BCPs are significantly closer to the H atoms (Figure 6). The lengths of both C–H bonds linked by the H···Ag hydrogen bond path undergo a slight increase in length of 0.002 Å compared with those in the optimized isolated ligand L^1 . Furthermore, the data listed in the second and third rows of Table 5 for the C–H···Ag close interactions exhibit the typical characteristic of closed-shell interactions: (a) a relatively low value for the density at the BCPs (ρ_b); (b) relatively small corresponding positive values for the Laplacian ($\nabla^2\rho_b$); (c) a positive value for the energy density H_b that is close to zero; and (d) the relationship $|\lambda_1|/\lambda_3 < 1$. In addition, the Laplacian of electron density, $\nabla^2\rho_b$, is positive, indicating that the interaction is dominated by the contraction of charge away from the interatomic surface toward each nucleus. The presence of intramolecular C–H···Ag hydrogen-bonding bond paths necessitates the formation of the ring structures (Ag(1)–H(5A)–C(5)–C(13)–N(1) and Ag(1)–H(4A)–C(4)–C(11)–N(1)) and the associated (3, 1) ring critical points (RCPs) ($\rho_r = 0.0110$ e au⁻³, $\nabla^2\rho_r = 0.0393$ e au⁻⁵ and $\rho_r = 0.0111$ e au⁻³, $\nabla^2\rho_r = 0.0401$ e au⁻⁵, respectively; Figure 6). We know that the physical presence of bonding between atoms denoted by the existence of a bond path will signify the presence of an accompanying energetic stabilization. Therefore, we semiquantitatively evaluate the strength of interaction related to the hydrogen bonds between H atoms and Ag ions by virtue of the energy difference of the two fragmental pairs ($Ag^+\cdots$ acridine and $Ag^+\cdots$ pyridine) intercepted from the optimized structure of **1** (see Scheme

(30) Reed, E.; Curtiss, L. A.; Weinhold, F. *Chem. Rev.* **1988**, *88*, 899.

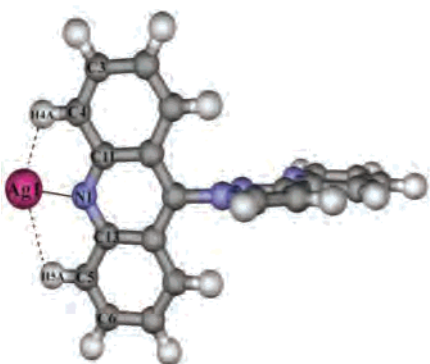
(31) All calculations were performed at the B3LYP/6-31++G** (Lan12dz for Ag) level of theory using the Gaussian 03 suite of programs. The topology of $\rho(r)_{\text{calcd}}$ was analyzed using the AIM98PC software package (ref 20).



(a)



(b)



(c)

Figure 6. View of (a) the total electron density, $\rho(r)$, and bond paths, (b) Laplacian charge density distributions for a fragment of **1** with optimized geometry in the plane defined by Ag(1), C(4), C(5), H(4A), and H(5A) (dashed contours denote positive values, solid contours denote negative values, solid circles denote the bond critical points (BCPs), blank circles denote the ring critical points (RCPs), and heavy solid lines denote the bond paths), and (c) schematic model graph of part of the molecule in **1** showing C–H...Ag H-bonding interactions (the locations of nuclei are labeled in (a) only for clarity).

1). The total interaction energy, including the basis set superposition errors (BSSE) correction using the counterpoise (CP) method,³² is estimated to be about 14 kJ/mol for the H...Ag weak interaction, which is very close to those values

(32) Boys, S. F.; Bernardi, F. *Mol. Phys.* **1970**, *19*, 553.

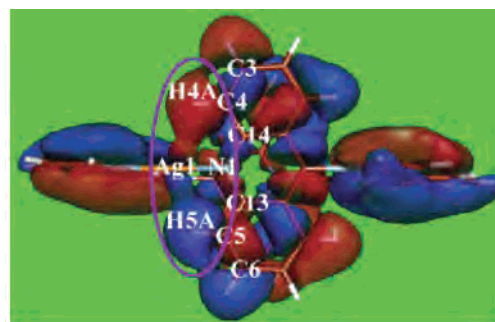
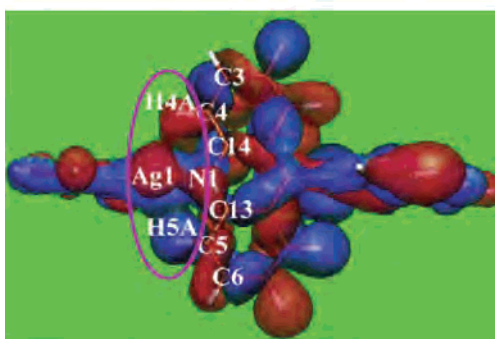
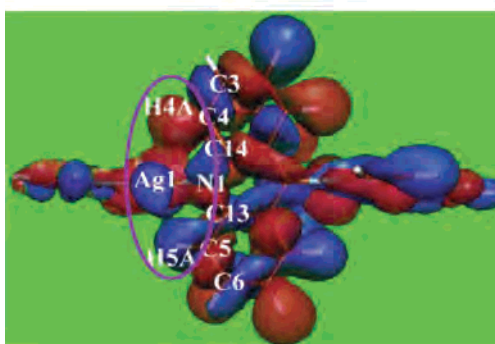
(a) 133rd(b) 150th(c) 152nd

Figure 7. Calculated molecular orbitals relevant to the C–H...Ag H-bonding interactions in **1** for the (a) 133rd, (b) 150th, and (c) 152nd molecular orbitals.

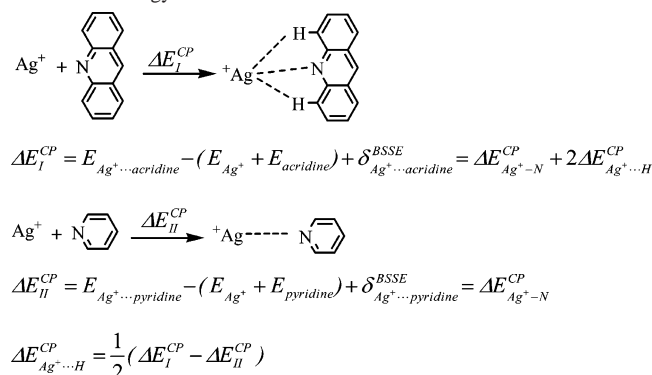
evaluated for C–H...O and C–H...N hydrogen bonds.^{16d,e,33} Thus, the C–H...Ag hydrogen-bonding interactions should be very important and strong enough to compete with other types of weak interactions in the construction of the coordination supramolecular systems.

On the other hand, NBO analysis also reveals that when L^1 coordinates to Ag(I) ions, the occupation numbers in the σ bonding orbitals of C(4)–H(4A) and C(5)–H(5A) decrease from 1.97844 and 1.97926 in the free ligand L^1 to 1.97523 and 1.97530 in **1**, respectively, whereas those of the σ^* antibonding orbital increase from 0.01167 and 0.01175 to 0.01505 and 0.01494, respectively. The changes in the occupation numbers suggest that electron transfer occurs

(33) Platts, J. A.; Howard, S. T.; Wozniak, K. *Chem. Phys. Lett.* **1995**, *232*, 479.

Table 5. Topological Properties of the Theoretically Calculated Charge Densities at the Selected Bond Critical Points of **1** (the values corresponding to the isolated free ligand **L**¹ are given in parentheses)

bond	length (Å)	d_1 (Å)	d_2 (Å)	ρ_b (e Å ⁻³)	$\nabla^2\rho_b$ (e Å ⁻⁵)	H_b (Hartree·Å ⁻³)	$ \lambda_1 /\lambda_3$
Ag(I)–N(1)	2.241	1.157	1.085	0.0672	0.2893	–0.0595	0.1754
Ag(I)⋯H(4A)	2.694	1.636	1.099	0.0110	0.0386	0.0101	0.1642
Ag(I)⋯H(5A)	2.686	1.630	1.091	0.0112	0.0391	0.0102	0.1644
C(4)–H(4A)	1.087	0.686	0.401	0.2839	–1.024	–2.0002	1.5805
	(1.085)	(0.688)	(0.396)	(0.2862)	(–1.047)	(–2.0301)	(1.5977)
C(5)–H(5A)	1.087	0.686	0.401	0.2839	–1.024	–2.0002	1.5808
	(1.085)	(0.687)	(0.398)	(0.2861)	(–1.045)	(–2.0280)	(1.5971)

Scheme 1. Illustration for the Evaluation of the Weak H⋯Ag Interaction Energy

from the σ bonding orbitals of C(4)–H(4A) and C(5)–H(5A) to the vacant orbitals of Ag(I) ions, together with back-transfer from filled metal d orbitals to the C(4)–H(4A) and C(5)–H(5A) σ^* antibonding orbitals, which is consistent with previous studies of some C–H⋯M hydrogen-bonding systems.^{17h,k} After investigations of all the occupied molecular orbitals (OMOs) of **1**, we found that the 133rd, 150th, and 152nd significantly contribute to the C–H⋯Ag weak interactions (Figure 7). It is clear that the atomic orbital overlap between H atoms and Ag centers can be observed from these molecular orbitals, which further confirms the presence of C–H⋯Ag close interactions in **1** from the viewpoints of electron transfer and atomic orbital overlap.

Concluding Remarks

In conclusion, four new Ag(I) supramolecular complexes in which **1**, **2**, and **4** exhibit rare C–H⋯Ag hydrogen-bonding interactions have been synthesized by reactions of Ag(I) salts with two well-designed rigid bulky acridine-based ligands. This work offers three new rare examples in which the N donors of the acridine rings coordinate to Ag(I) ions in coordination supramolecular systems. The full geometry optimization on the basis of the experimental structure, the

natural bond orbital (NBO), and topological property analyses using the AIM approach of the optimized structure for **1** were carried out by DFT calculations in comparison with X-ray diffraction, which gave further confirmation and a better understanding of the nature of the C–H⋯Ag weak interactions. The total interaction energy related to the hydrogen bonds between H and Ag(I) in **1** is evaluated to be about 14 kJ/mol for the H⋯Ag weak interaction, which is very close to those values estimated for C–H⋯O and C–H⋯N hydrogen bonds. In addition, NBO and MO analyses also confirm the presence of C–H⋯Ag weak interaction in **1**. These results strongly support the existence of the C–H⋯Ag hydrogen-bonding interactions in the coordination supramolecular systems, which may offer us an effective means for constructing unique supramolecular architectures via C–H⋯M close interactions (not only intramolecular but also intermolecular).

Acknowledgment. This work was supported by the National Science Funds for Distinguished Young Scholars of China (20225101) and NSFC (20373028, 20531040) and the high performance computing project of the Tianjin Commission of Science and Technology of China (043185111-5). The calculations were performed on a DeepComp 6800 supercomputer at CAS and a Nankai Stars supercomputer at Nankai University. We thank Dr. Fei Ding, Department of Chemistry, Nankai University, for helpful discussions on the ¹H NMR and 2D gCOSY spectra and we thank the reviewers for their valuable suggestions.

Supporting Information Available: Crystallographic information files (CIF) of complexes **1–4**; ¹H NMR spectra in CD₃CN solution of **L**¹, **L**², and complexes **1–3** (Figures S1 and S3–S6); 2D gCOSY spectrum in CD₃CN solution of **L**¹ (Figure S2); and mass spectra in ESI mode of complexes **1–3** (Figures S7–S9). This material is available free of charge via the Internet at <http://pubs.acs.org>.

IC060087A